Psychiatry Research: Neuroimaging 308 (2021) 111234

Contents lists available at ScienceDirect

Psychiatry Research: Neuroimaging

journal homepage: www.elsevier.com/locate/psychresns

White matter microstructure across brain-based biotypes for psychosis – findings from the bipolar-schizophrenia network for intermediate phenotypes

Sinead Kelly [a,b,*], Synthia Guimond [a,c], Ofer Pasternak [b], Olivia Lutz [a], Paulo Lizano [a], Suheyla Cetin-Karayumak [b], John A. Sweeney [d], Godfrey Pearlson [e], Brett A. Clementz [f], Jennifer E. McDowell [f], Carol A. Tamminga [g], Martha E. Shenton [b,h], Matcheri S. Keshavan [a]

[a] Department of Psychiatry, Beth Israel Deaconess Medical Center, Harvard Medical School, Boston, MA 02115, United States
[b] Department of Psychiatry, Brigham and Women's Hospital, Harvard Medical School, Boston, MA 02115, United States
[c] Department of Psychiatry, The Royal's Institute of Mental Health Research, University of Ottawa, Ottawa, ON K1Z 7K4, Canada
[d] Department of Psychiatry, University of Cincinnati, Cincinnati, OH 45221, United States
[e] Department of Psychiatry, Yale University, New Haven, CT 06520, United States
[f] Department of Psychology, University of Georgia, Athens, GA 30602, United States
[g] Department of Psychiatry, UT Southwestern Medical Center, Dallas, TX 75390, United States
[h] Department of Radiology, Brigham and Women's Hospital, Harvard Medical School, Boston, MA 02115, United States

A B S T R A C T

The B-SNIP consortium identified three brain-based Biotypes across the psychosis spectrum, independent of clinical phenomenology. To externally validate the Biotype model, we used free-water fractional volume (FW) and free-water corrected fractional anisotropy (FA_T) to compare white matter differences across Biotypes and clinical diagnoses. Diffusion tensor imaging data from 167 individuals were included: 41 healthy controls, 55 schizophrenia probands, 47 schizoaffective disorder probands, and 24 probands with psychotic bipolar disorder. Compared to healthy controls, FAt reductions were observed in the body of corpus callosum (BCC) for schizoaffective disorder ($d = 0.91$) and schizophrenia ($d = 0.64$). Grouping by Biotype, Biotype 1 showed FAt reductions in the CC and fornix, with largest effect in the BCC ($d = 0.87$). Biotype 2 showed significant FAt reductions in the BCC ($d = 0.90$). Schizoaffective disorder individuals had elevated FW in the CC, fornix and anterior corona radiata (ACR), with largest effect in the BCC ($d = 0.79$). Biotype 2 showed elevated FW in the CC, fornix and ACR, with largest effect in the BCC ($d = 0.94$). While significant diagnosis comparisons were observed, overall greater discrimination from healthy controls was observed for lower FAt in Biotype 1 and elevated FW in Biotype 2. However, between-group differences were modest, with one region (cerebral peduncle) showing a between-Biotype effect. No between-group effects were observed for diagnosis groupings.

1. Introduction

Schizophrenia, schizoaffective disorder, and psychotic bipolar disorder are severe neuropsychiatric disorders that cause functional disability and significant economic burden despite current treatments (Cloutier et al., 2016). It is therefore critical to attain a greater understanding of the etiology and biological underpinnings of these psychotic disorders. Major roadblocks in elucidating pathophysiology include the heterogeneity of clinical symptoms within each psychotic disorder as well as the similarities in clinical presentation between the disorders. Hence, clinical diagnoses incompletely capture biologically meaningful differences in individuals with psychosis (Tamminga et al., 2013).

In order to parse the neurobiological variance among the psychoses, the Bipolar and Schizophrenia Network for Intermediate Phenotypes (BSNIP) consortium has employed cognitive and neurophysiological measures that identify three neurobiologically distinct Biotypes, independent of clinical features (Tamminga et al., 2013). Biotype 1 cases had impaired cognition, low electrophysiological responses, poor psychosocial functioning, and high numbers of relatives for psychotic disorders. Biotype 2 cases had more modest but significant cognitive impairment, and high sensory-motor neural reactivity. Biotype 3 cases had nearly normal cognition and sensory-motor neural reactivity, the best psychosocial functioning, and the lowest rate of clinically affected relatives. In addition, Biotypes appear to differ in neurobiological measures that were not used in the construction of the Biotypes, including functional MRI (fMRI) and brain structural measures. Biotype 1 is typically characterised by greater alterations, with Biotype 3 being more comparable to healthy controls (Meda et al., 2012; Ivleva et al., 2017;

* Corresponding author at.
E-mail address: mkeshava@bidmc.harvard.edu (S. Kelly).

https://doi.org/10.1016/j.pscychresns.2020.111234
Received 21 May 2020; Received in revised form 22 October 2020; Accepted 1 December 2020
Available online 16 December 2020

Hudgens-Haney et al., 2018; Ji et al., 2020). Specifically, gray matter density loss is most extensive for Biotype 1, intermediate and more localized for Biotype 2, with small reductions for Biotype 3 (Ivleva et al., 2017). Similarly, Biotype 1 showed diminished intrinsic neural activity whereas Biotype 2 showed accentuated intrinsic activity and less deviant behavior whereas Biotype 3 showed no neurophysiological differences from healthy controls (Hudgens-Haney et al., 2018). Finally, widespread differences for Biotype-1 were observed in functional connectivity compare to healthy controls. Biotype-2 and Biotype-3 showed less functional connectivity differences (Ji et al., 2020). All methods were more sensitive in capturing brain differences in Biotypes compared to clinical diagnoses. Neurobiological characteristics of these subgroups could thus provide the basis for distinct molecular and therapeutic targets.

A common neuroimaging finding among psychotic disorders is disruption of white matter microstructure. Brain white matter abnormalities, such as lower fractional anisotropy (FA), have been detected in these disorders, as well as in first-degree relatives of people with psychosis (Kelly et al., 2018; Lu et al., 2011; Pezzoli et al., 2018). Diffusion tensor imaging (DTI) allows for the study of white in vivo, however, a range of biological pathologies may contribute to standard DTI measures, including extracellular free-water and axonal degeneration. Therefore standard DTI measures such as FA cannot distinguish the underlying biological contributors of white matter structural changes (Alexander et al., 2007; Assaf and Pasternak, 2008; Pierpaoli et al., 1996). An advanced diffusion imaging technique, free-water (FW) imaging, separates the contribution of freely diffusing water in extracellular space from water diffusing along the tissue and may offer increased sensitivity to detect microstructural differences (Pasternak et al., 2009). The free-water compartment is comprised of freely diffusing water molecules and is thought to be an indicator of extracellular changes that may be driven by pathologies such as neuroinflammation, atrophy, or edema (Pasternak et al., 2009). Previous studies have found localized free-water corrected FA (FAt) reductions in first-episode schizophrenia, accompanied by widespread elevated FW (Lyall et al., 2017; Pasternak et al., 2012a). A similar pattern of more widespread FW elevations are also observed in bipolar disorder (Tuozzo et al., 2018). Chronic schizophrenia, however, is found to be associated with more widespread FAt reductions and localized FW elevations, indicating white matter deterioration in chronic phases of the illness (Oestreich et al., 2017; Pasternak et al., 2015).

In the current study, we aimed to use this advanced white matter imaging technique as an additional approach for validating the B-SNIP Biotypes. More specifically, we examined white matter microstructure across the Biotypes, and investigated whether these Biotypes better discriminate white matter differences in individuals with psychotic disorders compared to symptom-based clinical diagnoses. Based on previous studies validating the Biotype model (Meda et al., 2012; Ivleva et al., 2017; Hudgens-Haney et al., 2018; Ji et al., 2019), we hypothesize that individuals in Biotype 1 and Biotype 2 will show greater differences in white matter microstructure, whereas Biotype 3 will show minimal differences, compared to healthy controls. We hypothesize that using conventional clinical diagnoses, individuals with schizophrenia, schizoaffective disorder, and psychotic bipolar disorder, will show white matter differences compared to controls, with schizophrenia and schizoaffective disorder showing the largest differences. Biotypes are hypothesized to show stronger between-group discrimination than conventional diagnosis.

2. Methods

2.1. Participants

Data included in this study were collected from 167 participants from two sites (Hartford, Baltimore) of the B-SNIP consortium: 41 healthy controls, 55 probands with schizophrenia, 47 probands with schizoaffective disorder, 24 probands with psychotic bipolar disorder (See Table 1Table 1). These data are from a subsample of participants included in Skudlarski et al. (2013), excluding first-degree relatives and those who did not have sufficient necessary data for a Biotype assignment. All participants provided written informed consent statements approved by review boards of Hartford Hospital/Yale University and the University of Maryland/Johns Hopkins University.

Consensus clinical diagnoses were established by trained clinical raters and senior psychiatric diagnosticians using clinical data and the Structured Clinical Interview for DSM-IV (SCID). The probands were clinically stable and had been taking stable doses of medications for at least 4 weeks. All bipolar participants had a history of psychosis during an affective episode (Meda et al., 2012). Symptoms severity was assessed by the Positive and Negative Syndrome Scale (PANSS) (Kay et al., 1987) and cognitive abilities was measured with the Brief Assessment of Cognition in Schizophrenia (BACS)(Keefe et al., 2004). Current psychosis status was judged according to scales of the Positive and Negative Syndrome Scale (PANSS) (Kay et al., 1987). The healthy controls did not have any current axis I disorders, as assessed by the SCID. All participants were free of known neurological illness, and were not actively using illicit substances reflected in negative urine toxicology screens. Though we strove to achieve balanced groups, matching was not exact. Our groups matched for age, however, there were significantly more males in the schizophrenia group compared to the other patient groups and healthy controls.

2.2. Diffusion weighted imaging acquisition

Diffusion weighted imaging data were obtained on 3-T scanners (Siemens, Erlangen, Germany). The scanners at Hartford (Allegra) and Baltimore (Trio) used the following scanning sequences; both used single-shot spin-echo planar imaging with a twice-refocused balance echo sequence to reduce eddy current distortions. Hartford used TR/TE = 6300/85 ms, field of view = 220 m, b = 1000 s/mm^2 along 32 directions, 45 contiguous slices, three imaging series, and a voxel size of 1.7 × 1.7 × 3 mm. Baltimore used TR/TE = 6700/92 ms, field of view = 230 m, b = 1000 s/mm^2 along 30 directions, 48 contiguous slices, two imaging series, and a voxel size of 1.8 × 1.8 × 3 mm.

2.3. Harmonization between sites

As the data were acquired across two sites with two different scanners, we utilized an harmonization technique that goes beyond meta-analyses and involves the signal of the magnet for harmonizing results from multiple cohorts. The harmonization analysis pipeline was implemented following the methods described in detail by Cetin-Karayumak et al. (2019). The technique harmonizes raw diffusion magnetic resonance imaging signal in a model-independent manner and aims to remove scanner related effects while preserving inter-subject biological variability and group differences across sites. A subset of age, diagnosis, and sex-matched participants (n = 20) were selected from both sites to create a template for harmonization. Raw diffusion magnetic resonance imaging data from Baltimore was then mapped onto the Hartford target reference site.

2.4. Diffusion weighted imaging preprocessing and FW imaging

Standard diffusion tensor imaging analysis techniques are unable to disentangle the contributions of partial volume effects, introducing bias to standard diffusion tensor imaging measures. FW is an advanced diffusion analysis technique (Pasternak et al., 2009) that separately models the contribution of extracellular FW and the one that is in the vicinity of the cellular tissue, named corrected fractional anisotropy (FAt). Differentiating these features provides more specific information relevant to underlying biological alterations. The FW Imaging analysis pipeline was implemented following the methods described in detail by

Table 1
Participant demographics.

Measure	SZ	SAD	BP	Biotype1	Biotype2	Biotype3	HC
N	55	47	24	32	42	52	41
N Hartford	26	32	15	13	30	30	19
N Baltimore	29	15	9	19	12	22	22
Mean Age (SD)	32.93 (10.03)	35.19 (11.42)	33.91 (12.82)	31.75 (10.23)	36.07 (11.91)	33.61 (10.80)	38.41 (11.52)
M:F	40:15	24:23	14:10	16:16	24:18	38:14	17:24
CPZ (mg)	524.55	499.63	381.35	503.90	501.53	473.22	NA
PANSS total	60.25	66.93	46.4	61.41	65.97	55.71	NA

Note: Healthy controls (HC), schizophrenia (SZ), schizoaffective disorder (SAD), and psychotic bipolar disorder (BP), Standard deviation (SD), Male (M), Female (F), Daily equivalence chlorpromazine (CPZ), Total Score on the Positive and Negative Syndrome Scale (PANSS).

Table 2
JHU white matter atlas regions.

Abbreviation	Full tract name
Average FW/FAt	Full skeleton average FW/FAt
ACR ($L + R$)	Anterior *corona radiata*
ALIC ($L + R$)	Anterior limb of internal capsule
BCC	Body of *corpus callosum*
CC (BCC+GCC+SCC)	Corpus callosum
CGC ($L + R$)	Cingulum (cingulate gyrus)
CGH ($L + R$)	Cingulum (hippocampal portion)
CR ($L + R$)	*Corona radiata*
CST ($L + R$)	Corticospinal tract
EC ($L + R$)	External capsule
FX	*Fornix*
FXST ($L + R$)	*Fornix* (cres) / *Stria terminalis*
GCC	***Genu*** of *corpus callosum*
IC ($L + R$)	Internal capsule
IFO ($L + R$)	Inferior fronto-occipital fasciculus
PCR ($L + R$)	Posterior *corona radiata*
PLIC ($L + R$)	Posterior limb of internal capsule
PTR ($L + R$)	Posterior thalamic radiation
RLIC ($L + R$)	Retrolenticular part of internal capsule
SCC	***Splenium*** of *corpus callosum*
SCR ($L + R$)	Superior *corona radiata*
SFO ($L + R$)	Superior fronto-occipital fasciculus
SLF ($L + R$)	Superior longitudinal fasciculus
SS ($L + R$)	Sagittal *stratum*
UNC ($L + R$)	*Uncinate* fasciculus

Note: $L + R$; averaged across left and right hemispheres.

Pasternak et al. (2009). First, diffusion weighted images (were corrected for motion and eddy-current artifacts. Masking of the diffusion weighted images was conducted using Otsu threshold masking in 3D Slicer (www.slicer.org; Fedorov et al., 2012; Kikinis et al., 2014). The FW and FAt maps were then generated by fitting the aligned diffusion weighted images with a two-compartment regularized model comprising a FW compartment and a tissue FAt compartment (Pasternak et al., 2009). The FW compartment accounts for the fractional volume of freely diffusing water molecules, expected in extracellular space whereas the tissue compartment accounts for the signal left after eliminating contribution of freely diffusing water. The FAt parameter enables more accurate estimations of tissue specific FA measures as the signal contribution from FW is attenuated. However, FW and the conventional FA measure should not necessarily be considered as mirror opposites. In the context of the FW model, regions with higher FW in the absence FAt reductions would be indicative of lower FA. However, if there is a reduction in FAt, without changes in FW, this would also be reflected as lower FA (Lyall et al., 2018).

2.5. White matter analysis

White matter was investigated using whole-brain tract-based spatial statistics (TBSS) A detailed description of the TBSS procedure is provided by Smith et al. (2006). A study specific template was created from the FA maps using ANTs (Advanced Normalization Tools (Avants et al., 2011)) multivariate template construction. FW and FAt images from all participants were registered to the template and each participant's aligned FW and FAt image was then projected onto a white matter skeleton creating a skeletonized FA map. White matter regions were defined according to the Johns Hopkins University white matter atlas calculating average FW and FAt for a total of 24 bilateral ROIs (Mori et al., 2008; Oishi et al., 2008) as well as average whole brain FAt and FW. The average FAt and FW within each of the 24 bilateral white matter region, averaged across left and right hemisphere, were then extracted (See Table 2).

2.6. Statistical analyses

All statistical analyses were conducted using R (version 3.5.1, https://www.r-project.org/). Demographic variables were assessed using t-tests and chi-squared tests. A series of general linear models were performed to investigate group differences for Biotype classification (4 levels: Healthy controls, Biotype 1, Biotype 2, Biotype 3) and clinical diagnosis (4 levels: Healthy controls, schizophrenia, schizoaffective disorder, psychotic bipolar disorder), for FAt and FW of bilateral ROIs, and effect sizes were calculated using Cohen's *d*. General linear models were also used to assess possible interactions between diagnoses and Biotypes. All analyses were controlled for age and sex. Site was not entered as a covariate, as recommended when data are harmonized between sites following the technique described above (Cetin Karayumak et al., 2019). All *p*-values were corrected using Bonferroni correction across 24 ROIs for group comparisons with an adjusted significance threshold of $p < .05$.

To further examine the neurobiological discrimination of Biotypes compared to conventional diagnoses, and to allow the comparison of both classification systems in one model, post-hoc logistic regressions were performed on significant ROIs to evaluate which subgroup classification (Biotype v conventional diagnosis) provided the optimal discrimination from healthy controls, as determined by the receiver operating characteristic (ROC) area under the curve (AUC). Finally, exploratory partial correlations, adjusting for age and sex, were calculated between FAt and FW measures for all ROIs, and available average daily chlorpromazine equivalent (CPZ) antipsychotic dose, PANSS total scores, and BACS total scores. All *p*-values were corrected using Bonferroni correction across 24 ROIs for group comparisons with an adjusted significance threshold of $p < .05$.

3. Results

3.1. Clinical diagnosis differences in FAt and FW

Of the 24 regions, significant FAt reductions were observed in individuals with schizoaffective disorder compared to healthy controls in the body of the corpus callosum (BCC) ($d = 0.91$, $p < .001$). Significant lower FAt was also seen in individuals with schizophrenia compared to healthy controls in the BCC ($d = 0.64$, $p = .03$). For FW, individuals with schizoaffective disorder had significantly elevated FW compared to healthy controls, with the largest effects observed for the BCC ($d = 0.78$), followed by the genu of the corpus callosum (GCC) ($d = 0.50$),

fornix, and anterior corona radiata (all p-values < 0.05 corrected; See Table 3 and Figs. 1 and 2).

3.2. Biotype differences in FAt and FW

Of the 24 regions, significant FAt reductions were seen in Biotype 1 probands compared to healthy controls, with the largest effects observed in BCC ($d = 0.90$, $p = .005$), followed by GCC ($d = 0.82$, $p = .03$), whole-brain average FAt ($d = 0.78$, $p = .007$) and fornix stria terminalis ($d = 0.79$, $p = .029$). Biotype 1 also showed lower FAt compared to Biotype 3 in the cerebral peduncle ($d = 0.72$, $p = .036$). Biotype 2 showed significant FAt reductions compared to healthy controls in the BCC ($d = 0.90$, $p < .001$). Biotype 3 did not significantly differ to healthy controls. (See Figs. 1 and 2 and Table 3). For FW, Biotype 2 showed significantly elevated FW compared to healthy controls in the BCC ($d = 0.94$), the GCC ($d = 0.90$), the splenium of the corpus callosum ($d = 0.73$), the fornix ($d = 0.73$) and the anterior corona radiate ($d = 0.68$). Biotype 3 also displayed elevated FW in the fornix (all p-values < 0.05 corrected; See Tables 3 and 4 and Figs. 1 and 2).

3.3. Biotype versus clinical diagnosis

For the BCC, the region with the largest effect size for group differences, post-hoc logistic regressions were performed to evaluate which subgroup classification (clinical diagnosis or Biotype) provided the optimal discrimination from healthy controls, as determined by the receiver operating characteristic (ROC) area under the curve (AUC).The AUC from the ROC analyses were used to assess the capacity to distinguish diagnostic or Biotype subgroups from healthy controls.

For FAt of the BCC, the following group discriminations were observed (AUC (standard error (SE)): Biotype 1 = 0.72 (0.061), Biotype 2 = 0.74 (0.056), Biotype 3 = 0.60 (0.059), schizophrenia = 0.63 (0.058), schizoaffective disorder =; 0.74 (0.054), psychotic bipolar disorder = 0.67 (0.070), with Biotype 2 and schizoaffective disorder demonstrating the greatest group discrimination compared to controls, followed by Biotype 1 (Fig. 3a).

For FW of the BCC, Biotypes 1, 2 and 3 were differentiated from healthy controls (AUC (SE)): Biotype 1 = 0.61 (0.069), Biotype 2 = 0.72 (0.055), Biotype 3 = 0.58 (0.060), and schizophrenia = 0.58 (0.059), schizoaffective disorder =; 0.69 (0.057, psychotic bipolar disorder = 0.64 (0.072), with Biotype 2 demonstrating the strongest group discrimination (Fig. 3b).

For widespread FAt differences across the white matter skeleton, Biotype 1 demonstrates the strongest group discrimination from healthy controls (AUC)(SE)): Biotype 1 = 0.65 (0.065), Biotype 2 = 0.55 (0.064), Biotype 3 = 0.53 (0.062), schizophrenia = 0.51 (0.061), schizoaffective disorder = 0.59 (0.062), psychotic bipolar disorder = 0.52 (0.076) (Fig. 4). Finally, no significant diagnosis-by-Biotype interactions were observed across ROIs.

Table 3
Significant clinical diagnosis group differences for FAt and FW measures.

Measure	Contrast	Region	Cohen's d	p-values adjusted
FAt	HC-SAD	BCC	0.91	.0004
FAt	HC-SZ	BCC	0.64	.03
FW	HC-SAD	ACR	0.67	.048
FW	HC-SAD	BCC	0.78	.01
FW	HC-SAD	FX	0.71	.04
FW	HC-SAD	GCC	0.71	.025
FW	HC-SZ	GCC	0.67	.03

Note: Free-water fractional volume (FW), free-water corrected fractional anisotropy (FA_T), healthy controls (HC), schizophrenia (SZ), schizoaffective disorder (SAD), body of corpus callosum (BCC), corpus callosum (GCC), fornix (FX), and anterior corona radiate (ACR).

Table 4
Significant biotype group differences for FAt and FW measures.

Measure	Contrast	Region	Cohen's d	p-values adjusted
FAt	Biotype1-HC	AverageFAt	0.79	.007
FAt	Biotype1-HC	BCC	0.87	.005
FAt	Biotype2-HC	BCC	0.90	.0005
FAt	Biotype1-Biotype3	CP	0.72	.03
FAt	Biotype1-HC	FX_ST	0.79	.02
FAt	Biotype1-HC	GCC	0.82	.03
FW	Biotype2-HC	ACR	0.68	.03
FW	Biotype2-HC	BCC	0.94	.001
FW	Biotype2-HC	FX	0.73	.03
FW	Biotype3-HC	FX	0.69	.04
FW	Biotype2-HC	GCC	0.90	.002
FW	Biotype2-HC	SCC	0.73	.01

Note: Free-water fractional volume (FW), free-water corrected fractional anisotropy (FA_T), healthy controls (HC), cerebral peduncle (CP), splenium of the corpus callosum (SCC), body of corpus callosum (BCC), corpus callosum (GCC), fornix (FX), and anterior corona radiate (ACR).

3.4. Association between FAt/FW and medication dose, symptom severity and cognition

After correction for multiple comparisons, no significant associations between FAt or FW, and CPZ or PANSS total scores were observed (all p-values > 0.05). A significant positive association between Average FAt and BACS total composite score was observed for healthy controls ($r = 0.44$, $p = .008$). No significant association between FAt or FW and cognition was observed for patients overall neither than for any Biotype or diagnosis groups (all p-values > 0.05).

4. Discussion

In the current study, we characterized Biotype and clinical diagnosis differences using advanced white matter measures. We hypothesized that individuals in Biotype 1 and Biotype 2 will show greater differences in white matter microstructure, whereas Biotype 3 will show minimal differences, compared to healthy controls. We hypothesize that using conventional clinical diagnoses, individuals with schizophrenia, schizoaffective disorder, and psychotic bipolar disorder, will show white matter differences compared to controls, with schizophrenia and schizoaffective disorder showing the largest differences. We also hypothesized that Biotypes would provide stronger between-group separation based on FW and FAt compared to conventional diagnoses.

In the current study, individuals with schizophrenia and schizoaffective disorders showed similar patterns of differences in FAt and FW compared to healthy controls, especially in BCC and GCC. Our findings show strongest and most widespread differences from healthy controls using Biotype grouping. Biotype 1 showed the largest effect for lower FAt compared to healthy controls in the BCC, GCC, FX_ST as well as across whole brain average FAt. Biotype 2 also showed lower FAt in the BCC. For FW, elevations were observed for SAD in the BCC, GCC, ACR and FX. When grouping by Biotype, Biotype 2 showed elevations in these regions, as well as the SCC, with larger effects in the BCC and GCC compared to effects observed when grouping by diagnosis. Logistic regressions of FW and FAt measures of the BCC suggest that Biotypes better differentiate FAt in the BCC from healthy controls, compared to diagnostic groups. For FW, Biotype 2 offered the best discrimination compared to all diagnostic groups.

Finally, although significant differences between Biotype groups were confined to one region (CP), the specificity and sensitivity to discriminate within subgroups of probands remains modest. No between-group effects for observed for diagnosis groupings. Hence, additional efforts are required to improve the identification of distinct subgroups of probands across the psychosis spectrum. Nevertheless, the Biotype model can be considered a step towards biological classification methods in psychosis and may identify subgroups of probands which are

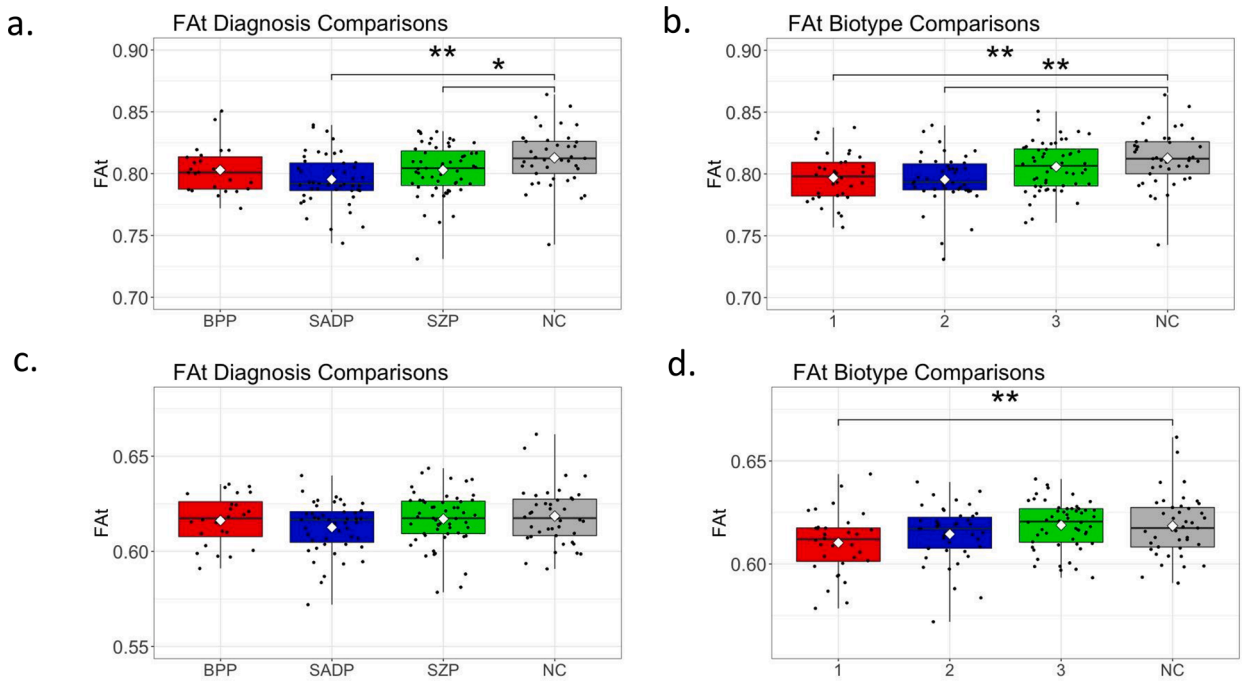

Fig. 1. FAt group differences for (a) Diagnosis groups for body of the corpus callosum (BCC), (b) Biotypes for BCC, (c) Diagnosis groups for average FAt across white matter skeleton (d) Biotypes for average FAt across white matter skeleton. Each dot represents data point for individual subject. Error bars represent 95% confidence interval; ** $p < .01$ Bonferroni corrected *$p < .05$ Bonferroni corrected; Healthy controls (NC), schizophrenia (SZP), schizoaffective disorder (SADP), and psychotic bipolar disorder (BPP).

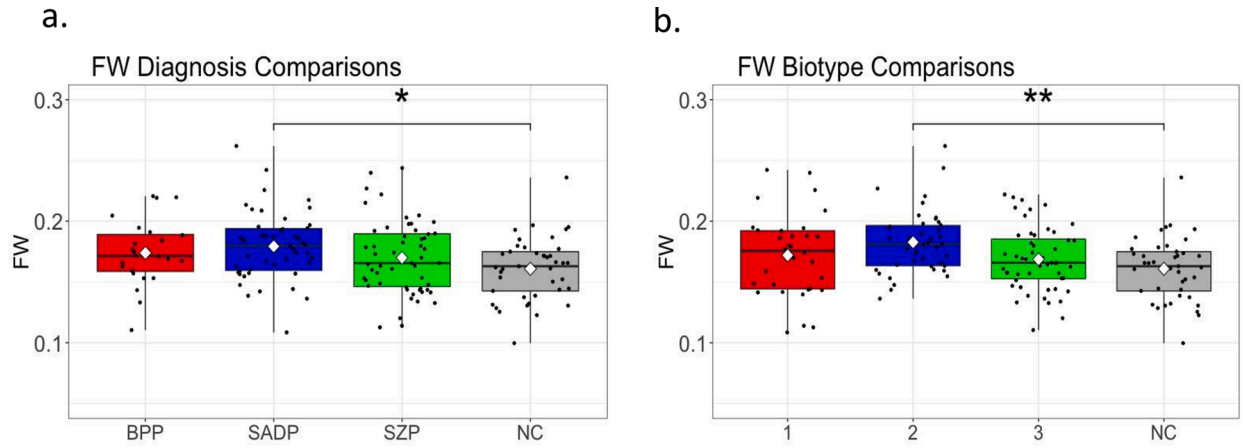

Fig. 2. FW group differences for a) DSM diagnosis groups in body of corpus callosum (BCC) and b) Biotypes in BCC. Each dot represents data point for individual subject. Error bars represent 95% confidence interval; ** $p < .01$ Bonferroni corrected *$p < .05$ Bonferroni corrected; Diagnosis group (DXGROUP), Healthy controls (NC), schizophrenia (SZP), schizoaffective disorder (SADP), and psychotic bipolar disorder (BPP).

biologically meaningful across the psychosis spectrum.

In all cases, individuals with psychotic bipolar disorder and those in Biotype 3 show the most similar FAt and FW profile to healthy controls. During the initial Biotype construction, Biotype 3 had relatively intact cognitive control and sensorimotor reactivity compared to healthy controls (Clementz et al., 2016). In addition, previous studies examining the external validators of these Biotypes found that gray matter is also similar between Biotype 3 and healthy controls, with the largest gray matter reductions reported for Biotype 1, followed by intermediate reductions in Biotype 2 (Ivleva et al., 2017). Finally, subtle differences in resting-state functional connectivity were observed in Biotype 3, whereas reduced connectivity was observed for Biotype 1 and Biotype 2 relative to Biotype 3 (Meda et al., 2016). Although Biotype 1 had the largest and most widespread effects for lower FAt, and Biotype 2 showed largest effects for elevated FW, no significant differences between Biotype 1 and Biotype 2 were observed. Similarly, resting-state functional connectivity findings revealed no significant differences between Biotypes 1 and 2 (Meda et al., 2016).

Finally, although significant differences between Biotype groups were confined to one region (CP), Biotype groupings better differentiate FAt and FW measures between probands and healthy controls. Logistic regressions of FW and FAt measures of the BCC suggest that Biotypes better differentiate FAt in the BCC from healthy controls, compared to diagnostic groups. For FW, Biotype 2 offered the best discrimination compared to all diagnostic groups. These are indications that the Biotype constructs may provide a proof of concept that differences based on brain-based biomarkers can regroup individuals with psychosis into neurobiologically distinct subgroups.

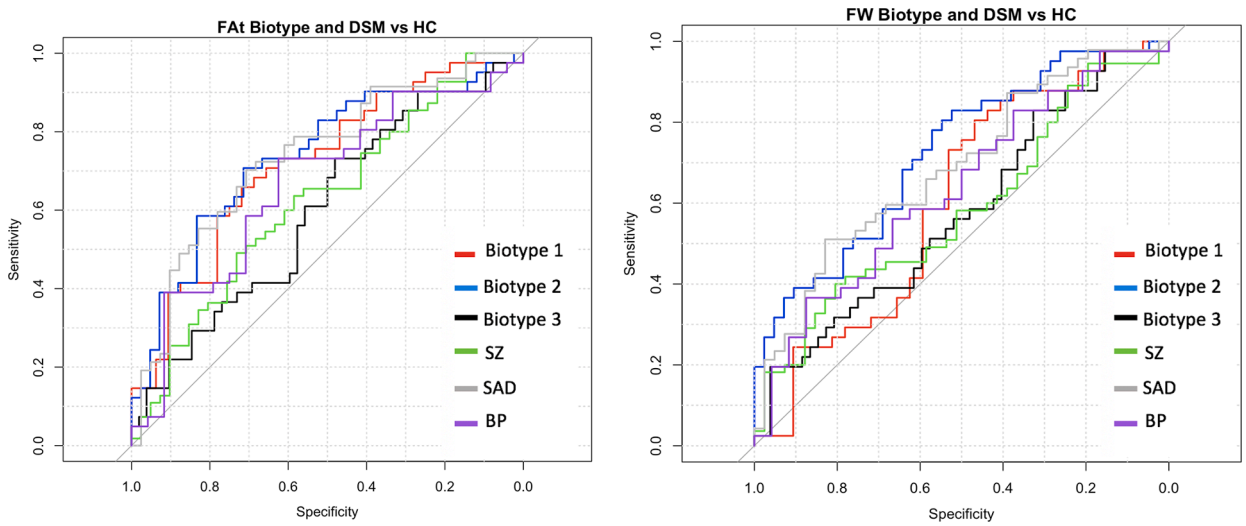

Fig. 3. Receiver operating curves for Biotype and diagnosis groups compared to healthy controls for (a) FAt of the BCC; Area Under the Curve (AUC)(standard error (SE)): Biotype 1 = 0.72 (0.061), Biotype 2 = 0.74 (0.056), Biotype 3 = 0.60 (0.059), schizophrenia = 0.63 (0.058), schizoaffective disorder =; 0.74 (0.054), psychotic bipolar disorder = 0.67 (0.070). (b) FW of the BCC; AUC (SE): Biotype 1 = 0.61 (0.069), Biotype 2 = 0.72 (0.055), Biotype 3 = 0.58 (0.060), and schizophrenia = 0.58 (0.059), schizoaffective disorder = 0.69 (0.057), psychotic bipolar disorder = 0.64 (0.072).

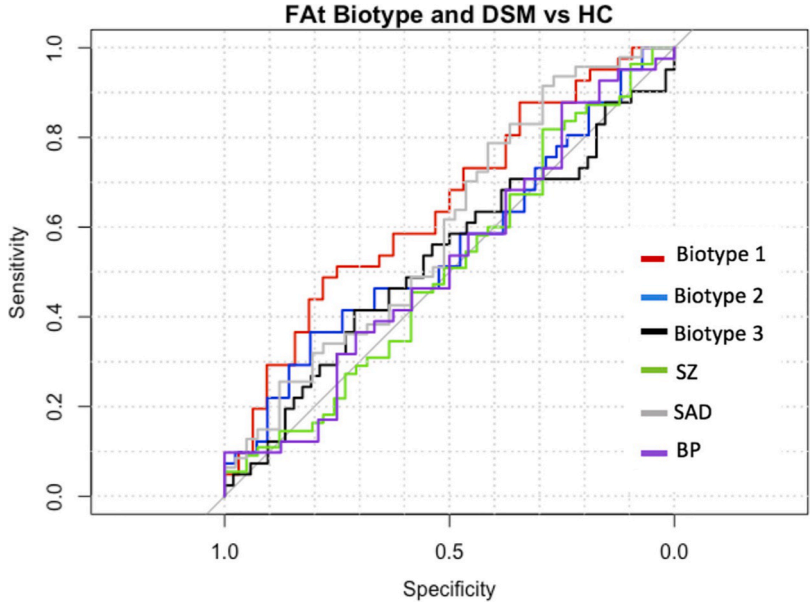

Fig. 4. Cloud sliding mode controller. (a) Structure diagram of sliding mode controller based cloud model. (b) cloud parameters. Receiver operating curves for Biotype and diagnosis groups compared to healthy controls for average whole-brain FAt; Area Under the Curve (AUC)(standard error (SE)): Biotype 1 = 0.65 (0.065), Biotype 2 = 0.55 (0.064), Biotype 3 = 0.53 (0.062), schizophrenia = 0.51 (0.061), schizoaffective disorder = 0.59 (0.062), psychotic bipolar disorder = 0.52 (0.076).

White matter alterations across Biotypes (i.e., primarily FAt decline in Biotype 1 and 2 in the BCC) may be related to the patterns of abnormalities previously observed for these Biotype groups in measures of neurocognition, gray matter, and resting-state functional connectivity (Ivleva et al., 2017; Meda et al., 2016; Clementz et al., 2016). Although we did not find a significant association between cognition and white matter in this sample, associations between white matter alterations and cognitive dysfunction have previously been reported in individuals with psychosis (Liu et al., 2015; Kochunov et al., 2017;). Future analyses in a larger sample for the second phase of this study will directly test the association between white matter measures, gray matter, functional connectivity and neurocognition in these Biotype groups. In addition, it is possible that localised FAt reductions and more widespread FW elevations for Biotype 2 probands may be related to the exaggerated sensorimotor reactivity characteristic of this Biotype (Clementz et al. 2016). For example, inhibitory deficits have previously been associated with lower FA across multiple white matter tracts in schizophrenia, including the BCC (Du et al., 2017). Future analyses will also directly test the associations between white matter measures and sensorimotor activity for these Biotypes. Elevated FW has also been reported in bipolar disorder and first-episode psychosis (Pasternak et al., 2012b; Tuozzo et al., 2018). It is possible that elevated FW, particularity in Biotype 2, may reflect state-related changes in this Biotype group, however; we found no significant differences in FW between individuals who were actively psychotic during scanning and those who were in remission. While elevated FW may indicate increased extracellular fractional volume (Pasternak et al., 2016), other pathologies such as decreased neuronal size (Rajkowska et al., 1998), which may be related

to FAt, or atrophy resulting from excessive synaptic pruning (Boksa, 2012), may also contribute to FW elevations. Future analyses are required to fully investigate the underlying pathologies associated with FW.

This study has limitations. First, the diffusion data was acquired using single-shell acquisition. Although single-shell data is permissible for FW estimation, multi-shell data provides an improved fit of the FW model. Second, the psychosis individuals in this study were in the chronic phases of psychosis and medicated. Therefore, disease burden and effects of medication on white matter measures could be potential confounds (Meng et al., 2019; Xiao et al., 2018). Although we could not control for lifetime medication and treatment effects in a cross-sectional sample, we did not find a significant association between FAt and FW measures and CPZ dose-equivalents at the time of scans in patients (see Table 1).

The Biotype model currently serves as a proof of concept requiring further validation, but these constructs may serve to complement clinical diagnoses by providing distinct groupings that are closer to underlying neurobiology. Although between-group effects are modest, the findings of this study show larger effects for lower FAt in Biotype 1 and elevated FW in Biotype 2 compared to healthy controls. Using an agnostic approach, such as Biotypes, may be particularly advantageous with regards to development of treatment targets, as well as assessing response to treatment, and may provide a pathway for individualized precision medicine in psychiatry.

Declaration of Competing Interest

J.A.S. is a scientific advisor for VeraSci, C.T is on the Advisory Board of Karuna and Kynexis and a DSB Member for Merck, as well as an ad hoc consultant for Sunovion and Astellas. All other authors reported no conflict of interest.

References

Alexander, A.L., Lee, J.E., Lazar, M., Field, A.S., 2007. Diffusion tensor imaging of the brain. Neurotherapeutics 4 (3), 316–329. https://doi.org/10.1016/j.nurt.2007.05.011.

Assaf, Y., Pasternak, O., 2008. Diffusion Tensor Imaging (DTI)-based white matter mapping in brain research: a review. J. Mol. Neurosci. 34 (1), 51–61. https://doi.org/10.1007/s12031-007-0029-0.

Avants, B. B., Tustison, N., & Song, G. (2011). *Advanced Normalization Tools* (ANTS). 35.

Boksa, P. (2012). Abnormal synaptic pruning in schizophrenia: urban myth or reality? *J. Psychiatry Neurosci.*, 37(2), 75–77. https://doi.org/10.1503/jpn.120007.

Cetin Karayumak, S., Bouix, S., Ning, L., James, A., Crow,, T., Shenton, M., Kubicki, M., Rathi, Y, 2019. Retrospective harmonization of multi-site diffusion MRI data acquired with different acquisition parameters. Neuroimage 184, 180–200. https://doi.org/10.1016/j.neuroimage.2018.08.073.

Clementz, B.A., Sweeney, J.A., Hamm, J.P., Ivleva, E.I., Ethridge, L.E., Pearlson, G.D., Keshavan, M.S., Tamminga, C.A., 2016. Identification of distinct psychosis biotypes using brain-based biomarkers. Am. J. Psychiatry 173 (4), 373–384. https://doi.org/10.1176/appi.ajp.2015.14091200.

Cloutier, M., Aigbogun, M.S., Guerin, A., Nitulescu, R., Ramanakumar, A.V., Kamat, S.A., DeLucia, M., Duffy, R., Legacy, S.N., Henderson, C., Francois, C., Wu, E., 2016. The Economic Burden of Schizophrenia in the United States in 2013. The Journal of Clinical Psychiatry 77 (6), 764–771. https://doi.org/10.4088/JCP.15m10278.

Du, X., Kochunov, P., Summerfelt, A., Chiappelli, J., Choa, F.-S., Hong, L.E., 2017. The role of white matter microstructure in inhibitory deficits in patients with schizophrenia. Brain Stimul. 10 (2), 283–290. https://doi.org/10.1016/j.brs.2016.11.006.

Fedorov, A., Beichel, R., Kalpathy-Cramer, J., Finet, J., Fillion-Robin, J.-C., Pujol, S., Bauer, C., Jennings, D., Fennessy, F., Sonka, M., Buatti, J., Aylward, S., Miller, J.V., Pieper, S., Kikinis, R., 2012. 3D slicer as an image computing platform for the quantitative imaging network. Magn. Reson. Imaging 30 (9), 1323–1341. https://doi.org/10.1016/j.mri.2012.05.001.

Hudgens-Haney, M.E., Ethridge, L.E., McDowell, J.E., Keedy, S.K., Pearlson, G.D., Tamminga, C.A., Keshavan, M.S., Sweeney, J.A., Clementz, B.A., 2018. Psychosis subgroups differ in intrinsic neural activity but not task-specific processing. Schizophr. Res. 195, 222–230. https://doi.org/10.1016/j.schres.2017.08.023.

Ivleva, E.I., Clementz, B.A., Dutcher, A.M., Arnold, S.J.M., Jeon-Slaughter, H., Aslan, S., Witte, B., Poudyal, G., Lu, H., Meda, S.A., Pearlson, G.D., Sweeney, J.A., Keshavan, M.S., & Tamminga, C.A. (2017). Brain structure biomarkers in the psychosis biotypes: findings from the Bipolar-Schizophrenia network for intermediate phenotypes. *Biol. Psychiatry*, 82(1), 26–39. https://doi.org/10.1016/j.biopsych.2016.08.030.

Ji, L., Meda, S.A., Tamminga, C.A., Clementz, B.A., Keshavan, M.S., Sweeney, J.A., Gershon, E.S., Pearlson, G.D., 2020. Characterizing functional regional homogeneity (ReHo) as a B-SNIP psychosis biomarker using traditional and machine learning approaches. Schizophr. Res. 215, 430–438. https://doi.org/10.1016/j.schres.2019.07.015.

Ji, L., Meda, S. A., Tamminga, C. A., Clementz, B. A., Keshavan, M. S., Sweeney, J. A., Gershon, E. S., & Pearlson,G. D. (2020). Characterizing functional regional homogeneity (ReHo) as a B-SNIP psychosis biomarker using traditional and machine learning approaches. *Schizophrenia Research*, 215.

Kay, S.R., Fiszbein, A., Opler, L.A., 1987. The Positive and Negative Syndrome Scale (PANSS) for Schizophrenia. Schizophr. Bull. 13 (2), 261–276. https://doi.org/10.1093/schbul/13.2.261.

Keefe, R.S.E., Goldberg, T.E., Harvey, P.D., Gold, J.M., Poe, M.P., Coughenour, L, 2004. The brief assessment of cognition in schizophrenia: reliability, sensitivity, and comparison with a standard neurocognitive battery. Schizophr. Res. 68 (2–3), 283–297. https://doi.org/10.1016/j.schres.2003.09.011.

Kelly, S., Jahanshad, N., Zalesky, A., Kochunov, P., Agartz, I., Alloza, C., Andreassen, O. A., Arango, C., Banaj, N., Bouix, S., Bousman, C.A., Brouwer, R.M., Bruggemann, J., Bustillo, J., Cahn, W., Calhoun, V., Cannon, D., Carr, V., Catts, S., Donohoe, G., 2018. Widespread white matter microstructural differences in schizophrenia across 4322 individuals: results from the ENIGMA Schizophrenia DTI Working Group. Mol. Psychiatry 23 (5), 1261–1269. https://doi.org/10.1038/mp.2017.170.

Kikinis, R., Pieper, S.D., Vosburgh, K.G., 2014. 3D Slicer: a platform for subject-specific image analysis, visualization, and clinical support. In: Jolesz, F.A. (Ed.), 3D Slicer: a platform for subject-specific image analysis, visualization, and clinical support. Intraoperative Imaging and Image-Guided Therapy 277–289. https://doi.org/10.1007/978-1-4614-7657-3_19.

Kochunov, P., Coyle, T.R., Rowland, L.M., Jahanshad, N., Thompson, P.M., Kelly, S., Du, X., Sampath, H., Bruce, H., Chiappelli, J., Ryan, M., Fisseha, F., Savransky, A., Adhikari, B., Chen, S., Paciga, S.A., Whelan, C.D., Xie, Z., Hyde, C.L., Hong, L.E., 2017. Association of White Matter With Core Cognitive Deficits in Patients With Schizophrenia. JAMA Psychiatry 74 (9), 958–966. https://doi.org/10.1001/jamapsychiatry.2017.2228.

Liu, C.-.C., Hua, M.-.S., Hwang, T.-.J., Chiu, C.-.Y., Liu, C.-.M., Hsieh, M.H., Chien, Y.-.L., Lin, Y.-.T., Hwu, H.-.G., 2015. Neurocognitive functioning of subjects with putative pre-psychotic states and early psychosis. Schizophr. Res. 164 (1–3), 40–46. https://doi.org/10.1016/j.schres.2015.03.006.

Lu, L.H., Zhou, X.J., Keedy, S.K., Reilly, J.L., Sweeney, J.A., 2011. White matter microstructure in untreated first episode bipolar disorder with psychosis: comparison with schizophrenia. Bipolar Disord 13 (7–8), 604–613. https://doi.org/10.1111/j.1399-5618.2011.00958.x.

Lyall, A.E., Pasternak, O., Robinson, D.G., Newell, D., Trampush, J.W., Gallego, J.A., Fava, M., Malhotra, A.K., Karlsgodt, K.H., Kubicki, M., Szeszko, P.R., 2017. Greater extracellular free-water in first-episode psychosis predicts better neurocognitive functioning. Mol. Psychiatry 23, 701.

Lyall, A.E., Pasternak, O., Robinson, D.G., Newell, D., Trampush, J.W., Gallego, J.A., Fava, M., Malhotra, A.K., Karlsgodt, K.H., Kubicki, M., Szeszko, P.R., 2018. Greater extracellular free-water in first-episode psychosis predicts better neurocognitive functioning. Mol. Psychiatry 23 (3), 701–707. https://doi.org/10.1038/mp.2017.43.

Meda, S.A., Clementz, B.A., Sweeney, J.A., Keshavan, M.S., Tamminga, C.A., Ivleva, E.I., Pearlson, G.D., 2016. Examining functional resting-state connectivity in psychosis and its subgroups in the bipolar-schizophrenia network on intermediate phenotypes cohort. Biol Psychiatry Cogn. Neurosci. Neuroimaging 1 (6), 488–497. https://doi.org/10.1016/j.bpsc.2016.07.001.

Meda, S.A., Gill, A., Stevens, M.C., Lorenzoni, R.P., Glahn, D.C., Calhoun, V.D., Sweeney, J.A., Tamminga, C.A., Keshavan, M.S., Thaker, G., Pearlson, G.D., 2012. Differences in resting-state fMRI functional network connectivity between schizophrenia and psychotic bipolar probands and their unaffected first-degree relatives. Biol. Psychiatry 71 (10), 881–889. https://doi.org/10.1016/j.biopsych.2012.01.025.

Meng, L., Li, K., Li, W., Xiao, Y., Lui, S., Sweeney, J.A., Gong, Q., 2019. Widespread white-matter microstructure integrity reduction in first-episode schizophrenia patients after acute antipsychotic treatment. Schizophr. Res. 204, 238–244. https://doi.org/10.1016/j.schres.2018.08.021.

Mori, S., Oishi, K., Jiang, H., Jiang, L., Li, X., Akhter, K., Hua, K., Faria, A.V., Mahmood, A., Woods, R., Toga, A.W., Pike, G.B., Neto, P.R., Evans, A., Zhang, J., Huang, H., Miller, M.I., van Zijl, P., Mazziotta, J., 2008. Stereotaxic white matter atlas based on diffusion tensor imaging in an ICBM template. Neuroimage 40 (2), 570–582. https://doi.org/10.1016/j.neuroimage.2007.12.035.

Oestreich, L.K.L., Lyall, A.E., Pasternak, O., Kikinis, Z., Newell, D.T., Savadjiev, P., Bouix, S., Shenton, M.E., Kubicki, M., Whitford, T.J., McCarthy-Jones, S, 2017. Characterizing white matter changes in chronic schizophrenia: a free-water imaging multi-site study. Schizophr. Res. 189, 153–161. https://doi.org/10.1016/j.schres.2017.02.006.

Oishi, K., Zilles, K., Amunts, K., Faria, A., Jiang, H., Li, X., Akhter, K., Hua, K., Woods, R., Toga, A.W., Pike, G.B., Rosa-Neto, P., Evans, A., Zhang, J., Huang, H., Miller, M.I., van Zijl, P.C.M., Mazziotta, J., Mori, S., 2008. Human brain white matter atlas: identification and assignment of common anatomical structures in superficial white matter. Neuroimage 43 (3), 447–457. https://doi.org/10.1016/j.neuroimage.2008.07.009.

Pasternak, O., Kubicki, M., Shenton, M.E., 2016. In vivo Imaging of Neuroinflammation in Schizophrenia. Schizophr. Res. 173 (3), 200–212. https://doi.org/10.1016/j.schres.2015.05.034.

Pasternak, O., Sochen, N., Gur, Y., Intrator, N., Assaf, Y., 2009. Free water elimination and mapping from diffusion MRI. Magn Reson Med 62 (3), 717–730. https://doi.org/10.1002/mrm.22055.

Pasternak, O., Westin, C.-.F., Bouix, S., Seidman, L.J., Goldstein, J.M., Woo, T.-U.W., Petryshen, T.L., Mesholam-Gately, R.I., McCarley, R.W., Kikinis, R., Shenton, M.E., Kubicki, M., 2012a. Excessive extracellular volume reveals a neurodegenerative pattern in schizophrenia onset. J. Neurosci. 32 (48), 17365. https://doi.org/10.1523/JNEUROSCI.2904-12.2012.

Pasternak, O., Westin, C.-.F., Bouix, S., Seidman, L.J., Goldstein, J.M., Woo, T.-U.W., Petryshen, T.L., Mesholam-Gately, R.I., McCarley, R.W., Kikinis, R., Shenton, M.E., & Kubicki, M. (2012b). Excessive extracellular volume reveals a neurodegenerative pattern in schizophrenia onset. *J. Neurosci*, 32(48), 17365–17372. https://doi.org/10.1523/JNEUROSCI.2904-12.2012.

Pasternak, O., Westin, C.-.F., Dahlben, B., Bouix, S., Kubicki, M., 2015. The extent of diffusion MRI markers of neuroinflammation and white matter deterioration in chronic schizophrenia. White Matter Pathology 161 (1), 113–118. https://doi.org/10.1016/j.schres.2014.07.031.

Pezzoli, S., Emsell, L., Yip, S.W., Dima, D., Giannakopoulos, P., Zarei, M., Tognin, S., Arnone, D., James, A., Haller, S., Frangou, S., Goodwin, G.M., McDonald, C., Kempton, M.J., 2018. Meta-analysis of regional white matter volume in bipolar disorder with replication in an independent sample using coordinates, T-maps, and individual MRI data. Neurosci. Biobehav. Rev. 84, 162–170. https://doi.org/10.1016/j.neubiorev.2017.11.005.

Pierpaoli, C., Jezzard, P., Basser, P.J., Barnett, A., Di Chiro, G., 1996. Diffusion tensor MR imaging of the human brain. Radiology 201 (3), 637–648. https://doi.org/10.1148/radiology.201.3.8939209.

Rajkowska, G., Selemon, L.D., Goldman-Rakic, P.S., 1998. Neuronal and glial somal size in the prefrontal cortex: a postmortem morphometric study of schizophrenia and Huntington disease. Arch. Gen. Psychiatry 55 (3), 215–224. https://doi.org/10.1001/archpsyc.55.3.215.

Skudlarski, P., Schretlen, D.J., Thaker, G.K., Stevens, M.C., Keshavan, M.S., Sweeney, J. A., Tamminga, C.A., Clementz, B.A., O'Neil, K., Pearlson, G.D, 2013. Diffusion tensor imaging white matter endophenotypes in patients with schizophrenia or psychotic bipolar disorder and their relatives. Am. J. Psychiatry 170 (8), 886–898. https://doi.org/10.1176/appi.ajp.2013.12111448.

Smith, S.M., Jenkinson, M., Johansen-Berg, H., Rueckert, D., Nichols, T.E., Mackay, C.E., Watkins, K.E., Ciccarelli, O., Cader, M.Z., Matthews, P.M., Behrens, T.E.J., 2006. Tract-based spatial statistics: voxelwise analysis of multi-subject diffusion data. Neuroimage 31 (4), 1487–1505. https://doi.org/10.1016/j.neuroimage.2006.02.024.

Tamminga, C.A., Ivleva, E.I., Keshavan, M.S., Pearlson, G.D., Clementz, B.A., Witte, B., Morris, D.W., Bishop, J., Thaker, G.K., Sweeney, J.A., 2013. Clinical phenotypes of psychosis in the Bipolar-Schizophrenia Network on Intermediate Phenotypes (B-SNIP). Am. J. Psychiatry 170 (11), 1263–1274. https://doi.org/10.1176/appi.ajp.2013.12101339.

Tuozzo, C., Lyall, A.E., Pasternak, O., James, A.D.C., Crow, T.J., Kubicki, M, 2018. Patients with chronic bipolar disorder exhibit widespread increases in extracellular free water. Bipolar Disord. 20 (6), 523–530. https://doi.org/10.1111/bdi.12588.

Xiao, Y., Sun, H., Shi, S., Jiang, D., Tao, B., Zhao, Y., Zhang, W., Gong, Q., Sweeney, J.A., Lui, S., 2018. White matter abnormalities in never-treated patients with long-term schizophrenia. Am. J. Psychiatry 175 (11), 1129–1136. https://doi.org/10.1176/appi.ajp.2018.17121402.